Crustal structure of the Mendeleev Rise and the Chukchi Plateau (Arctic Ocean) along the Russian wide-angle and multichannel seismic reflection experiment “Arctic-2012”

Kashubin, Sergey; Petrov, Oleg; Artemieva, Irina; Morozov, Andrey; Vyatkina, D.V.; Golysheva, Yu.S.; Kashubina, T.V. ; Milshtein, E.D. ; Rybalka, A.V. ; Erinchek, Yu.M. ; Sakulina, T.S. ; Krupnova, N.A.; Shulgin, A.A.

Published in:
Journal of Geodynamics

DOI:
10.1016/j.jog.2018.03.006

Publication date:
2018

Document version
Publisher's PDF, also known as Version of record

Journal of Geodynamics 119 (2018) 107–122

Contents lists available at ScienceDirect

Journal of Geodynamics

journal homepage: www.elsevier.com/locate/jog

Crustal structure of the Mendeleev Rise and the Chukchi Plateau (Arctic Ocean) along the Russian wide-angle and multichannel seismic reflection experiment "Arctic-2012"

S.N. Kashubin[a], O.V. Petrov[a], I.M. Artemieva[b], A.F. Morozov[c], D.V. Vyatkina[a], Yu.S. Golysheva[a], T.V. Kashubina[a], E.D. Milshtein[a], A.V. Rybalka[a,*], Yu.M. Erinchek[a], T.S. Sakulina[d], N.A. Krupnova[a,d], A.A. Shulgin[e]

[a] A.P. Karpinsky Russian Geological Research Institute (VSEGEI), St.-Petersburg, Russia
[b] IGN, University of Copenhagen, Denmark
[c] Russian Federal Agency for Mineral Resources (Rosnedra), Moscow, Russia
[d] JSC Sevmorgeo,St.-Petersburg, Russia
[e] CEED, University of Oslo, Norway,

ARTICLE INFO

Keywords:
Magmatic underplating
Submarine continental plateau
Serpentinization
Wide-angle marine seismics
Ray-tracing
Gravity modeling

ABSTRACT

We present a seismic and density model for the crust and the uppermost mantle of the Arctic Ocean off-shore Chukotka down to a 40 km depth along a 740-km long latitudinal (at ca. 77°N) "Arctic-2012" wide-angle/MCS profile. Joint seismic and gravity modeling indicates significant differences in the crustal velocity and density structure of the northeastern Vilkitsky Trough, the Mendeleev Rise, the Chukchi Basin, and the Chukchi Plateau.

The Vilkitsky Trough and the Chukchi Basin have a thin crust (23 km and 18 km, correspondingly), 6–8 km thick sedimentary cover, 3–6 km thick upper/middle crust (with the smallest thickness of 3–4 km beneath the Chukchi Basin), and 9–10 km thick lower crust. The uppermost mantle of the Chukchi Basin has a high density (3.27–3.31 g/cm^3) and a low velocity (Vp ~ 7.8 km/s), which we explain by 5–10% serpentinization of mantle peridotite at a 22–35 km depth as a result of crustal hyperextension and seawater penetration.

The Chukchi Plateau and the Mendeleev Rise have a thick crust (28–29 km and 33–34 km, correspondingly), underlain by a normal mantle (Vp ~ 8.0 km/s). The Chukchi Plateau has a 2-4 km thick sedimentary cover, a thick (15–18 km) upper/middle crust with low-Vp, low-density lenses interpreted as magmatic intrusions, and a 9–12 km thick lower crust. The Mendeleev Rise has a 3–7 km thick sedimentary cover (most of which is formed by metasediments with a possible presence of volcanic rocks), a 7–8 km thick upper/middle crust, and a thick (20 km) lower crust which includes a 3–4 km thick high-velocity (Vp ~ 7.3 km/s) underplated magmatic material. The high density anomaly (at depths > 35 km) below the Mendeleev Rise is interpreted as an eclogitic body in the upper mantle lithosphere.

Seismic Vp and Vp/Vs structure of the crust along the "Arctic-2012" profile indicates its continental nature: a 3–18 km thick upper/middle crustal layer with Vp ~ 6.0–6.8 km/s and Vp/Vs ~ 1.70–1.73 typical of felsic-intermediate continental upper crust is present along the entire profile. Strong variability of the crustal structure along the profile reflects its significant modification by metamorphism and magmatism, possibly related to the High-Arctic Large Igneous Province and localized lithosphere extension beneath the Chukchi Basin.

1. Introduction

Tectonic origin of the system of the Alpha-Mendeleev submarine rises/ridges (AMSR) of the Arctic Ocean is still debated (Lane and Stephenson, 2016). Both bathymetric highs, which form a ca. 2000 km × 400 km submarine elevation with a depression in the middle (the Cooperation Gap separating the Mendeleev Rise and the Alpha Ridge, Fig. 1a), are usually interpreted to result from the same

* Corresponding author.
E-mail addresses: Sergey_Kashubin@vsegei.r (S.N. Kashubin), OPetrov@vsegei.ru (O.V. Petrov), Irina@ign.ku.dk (I.M. Artemieva), AMorozov@rosnedra.com (A.F. Morozov), Darya_Vyatkina@vsegei.ru (D.V. Vyatkina), Juliya_Golysheva@vsegei.ru (Y.S. Golysheva), Tatiana_Kashubina@vsegei.ru (T.V. Kashubina), Evgenia_Milshtein@vsegei.ru (E.D. Milshtein), Alexander_Rybalka@vsegei.ru (A.V. Rybalka), Yuri_Erinchek@vsegei.ru (Y.M. Erinchek), Sakoulina@gmail.com (T.S. Sakulina), N_Krupnova@mail.ru (N.A. Krupnova), Alexey.Shulgin@geo.uio.no (A.A. Shulgin).

https://doi.org/10.1016/j.jog.2018.03.006
Received 2 August 2017; Received in revised form 2 March 2018; Accepted 20 March 2018
Available online 23 March 2018

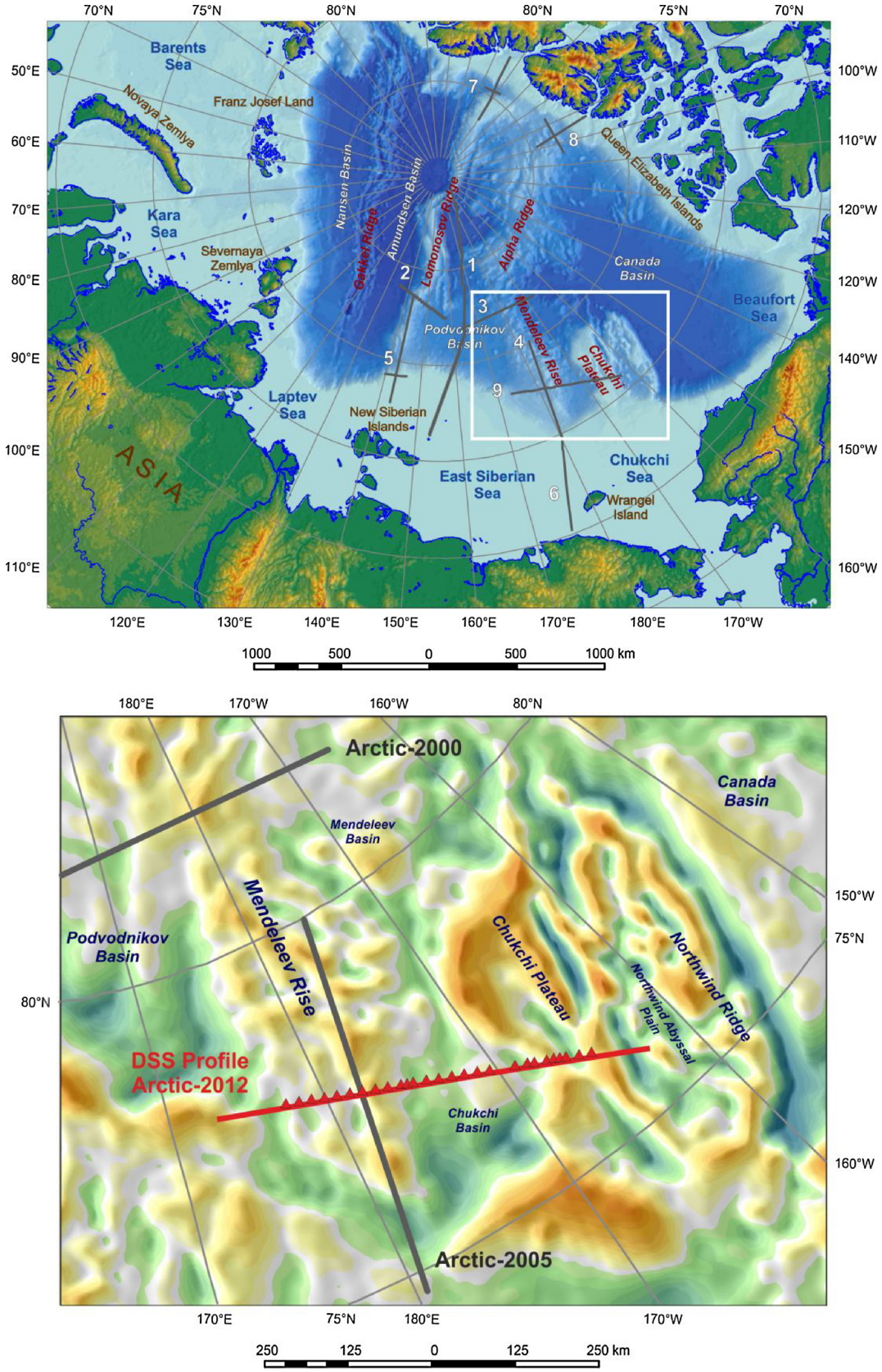

Fig. 1. Wide-angle profiles in the area of the Central Arctic uplifts (top panel) and location of the "Arctic-2012" wide-angle profile plotted on the map of free air gravity anomalies in the Circumpolar Arctic (Gaina et al., 2011) (bottom panel). Wide-angle profiles (top panel): 1–Transarctic-89-91 (Poselov et al., 2011; Lebedeva-Ivanova et al., 2011); 2–Transarctic-92 (Poselov et al., 2011); 3–Arctic-2000 (Poselov et al., 2011; Lebedeva-Ivanova et al., 2006); 4–Arctic-2005 (Poselov et al., 2011); 5–Arctic-2007 (Poselov et al., 2011); 6–5-AR (Sakulina et al., 2011); 7–Lorita (Jackson et al., 2010); 8–ARTA (Funck et al., 2011); 9–Arctic-2012 (this study). Red triangles in the bottom panel – OBS locations for the "Arctic-2012" profile.

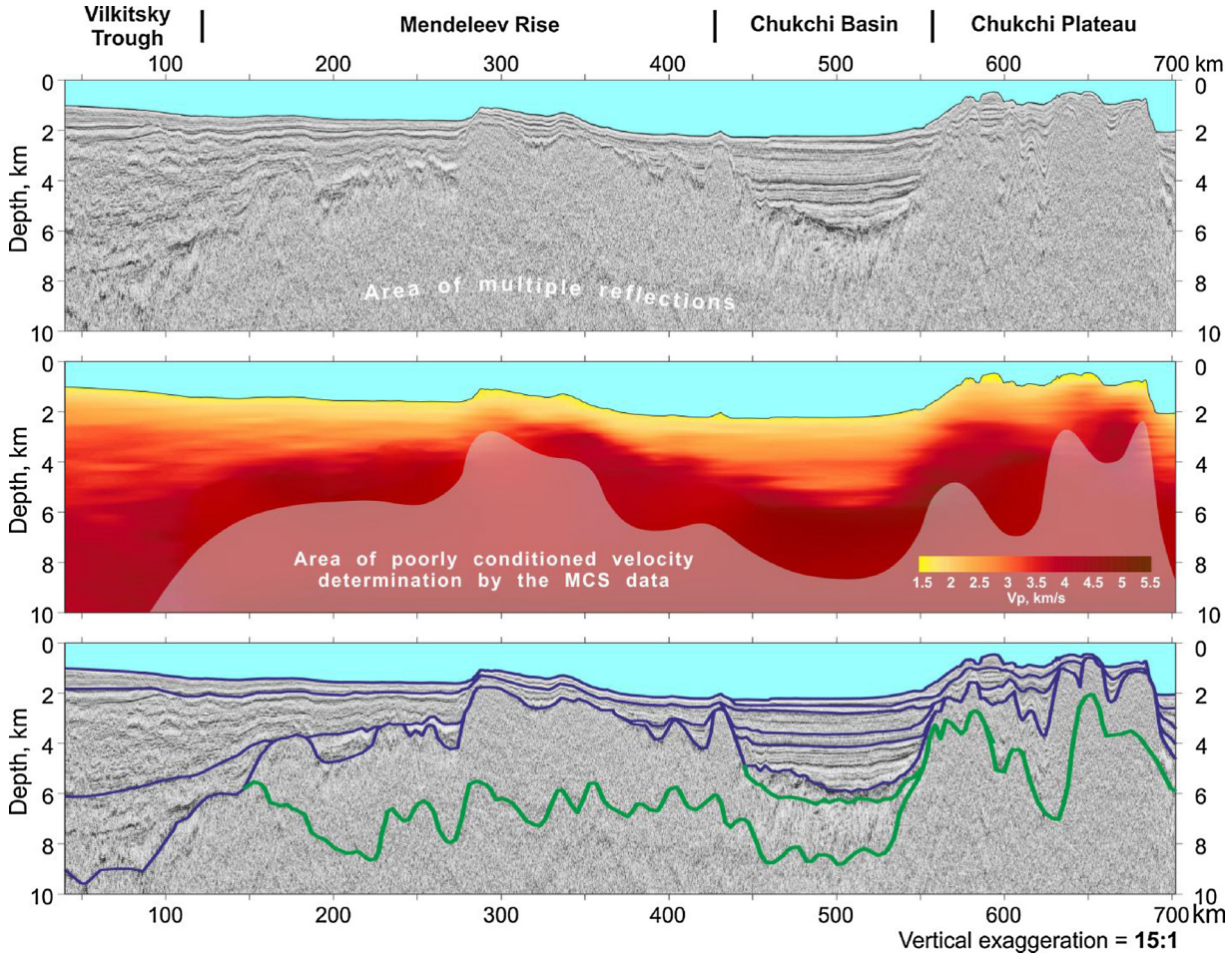

Fig. 2. MCS reflection depth section (upper panel), velocity model from the MCS data (middle panel), and seismic boundaries determined from the wide-angle data plotted atop of the MCS section (lower panel). Blue lines – boundaries determined from the wide-angle data coinciding with interfaces from the MCS data, green line – boundary constrained only from the wide-angle data.

tectonic processes, such as for example modification of a continental plateau by LIP-related volcanism with the Kerguelen Plateau as a possible closest analogue (Oakey and Saltus, 2016). Elucidation of geodynamic relationship between these bathymetric highs and their relationship to the adjacent geological structures remains a matter of debate, although many studies are inclined to extrapolate results of geological and geophysical studies of a part of the submarine elevation system to the entire system of the bathymetric highs. Three most common viewpoints on the nature of the Alpha-Mendeleev system are the following:

(1) AMSR is an oceanic plateau formed by long-lasting and probably hotspot-related volcanic eruptions in the Late Cretaceous (similar to the Iceland hotspot) (Forsyth et al., 1986; Jokat, 2003; Funck et al., 2011);
(2) AMSR is a rifted continental volcanic margin (White and McKenzie, 1989; Coffin and Eldholm, 1994; Dove et al., 2010);
(3) AMSR is a submerged system of uplifts formed on the continental crust (similar to the Lomonosov Ridge crust) intensively modified by subsequent, possibly plume-related, magmatism (Miller et al., 2006; Lebedeva-Ivanova et al., 2006; Poselov et al., 2011; Oakey and Saltus, 2016).

Despite a significant diversity of the opinions on the geological and tectonic origin of the AMRS crust, all studies agree that its original structure has been significantly modified by an extensive volcanism and magmatism. Geological and geophysical information on the structure of the AMSR has increased significantly over the past 15 years, in particular due to research efforts by the Arctic states (first of all by Denmark, Canada, and Russia) aimed at establishing the boundaries of their continental shelves in the Arctic Ocean. Recent Arctic surveys included seismic surveys from manned drifting ice research stations, multichannel seismic (MCS) near-vertical-incidence reflection surveys from research vessels escorted by powerful icebreakers, and wide-angle seismic reflection and refraction studies. These surveys made it possible to determine seismic velocity structure of the crust in different tectonic provinces of the Arctic ocean; however the number of crustal-scale seismic models for the AMRS remains limited (e.g. Lebedeva-Ivanova et al., 2006; Poselov et al., 2007, 2011; Funck et al., 2011; Sakulina et al., 2011) (Fig. 1).

The combined high-latitude geological and geophysical expedition “Arctic-2012” (Morozov et al., 2014) has acquired seismic data along a 740-km long latitudinal line crossing the Mendeleev Rise at about 77°N (across the northeastern Vilkitsky Trough, the Mendeleev Rise, the Chukchi Basin, and the Chukchi Plateau) (Fig. 1). The “Arctic-2012” seismic survey included wide-angle profile with autonomous ocean bottom seismometers (OBS) and multichannel seismic (MCS) reflection survey with a towed streamer. At present, this is the most high-latitude wide-angle seismic line on the Mendeleev Rise performed with OBS and multicomponent records (earlier, wide-angle studies at these latitudes were performed with on-land vertical seismometers deployed on ice).

Here we present results of seismic interpretation and joint seismic and gravity modeling along the “Arctic-2012” wide-angle profile, which includes seismic Vp, Vp/Vs and density model for the crust and the

uppermost mantle of the Mendeleev Rise, the Vilkitsky Trough, the Chukchi Basin, and the Chukchi Plateau. We compare regional crustal structure with seismic structure of other parts of the Arctic ocean, and provide evidence for the continental nature of the crust of the Mendeleev Rise and the adjacent tectonic units along the profile.

2. Data

2.1. "Arctic-2012" seismic data acquisition

Seismic OBS and MCS data were acquired in August-September 2012 by JSC Sevmorgeo from the *Dixon* diesel icebreaker (Morozov et al., 2014).

1) The wide-angle survey used a single high-power 7320 cub. in. (120 l) SIN–6 M airgun with shot spacing of 315 m and 27 ocean bottom seismometers (OBS) equipped with a three-component geophone and a hydrophone. The OBS spacing ranged from 10 km to 20 km with the maximum distance between the outermost instruments of 480 km. The total length of the wide-angle line is 740 km (shooting was extended for 130 km in each direction from the outermost OBSs).
2) The MCS reflection surveys along the wide-angle profile (contractor – WGP Exploration Limited, U.K.) were conducted with the 4500 m long 360-channel towed *Sercel SEAL* streamer (12.5 m channel spacing). Bolt APG airgun array with the total volume of 2050 cu in (33.6 *l*) operating at pressures of 135–145 bar was used as a seismic source. The shooting interval was 50 m resulting in the common midpoint (CMP) fold of 45.

The details on seismic data processing are described in Appendix A. Fig. 2 shows the seismic depth section of the upper crust along the MCS profile combined with interfaces obtained from the wide-angle data modeling.

2.2. Wide-angle data

In general, seismic records along the "Arctic-2012" wide-angle profile are of high quality (see Figs. S1-S3 in the Electronic Supplementary Data Section). Refracted waves in the sediments (Psed), crystalline basement (Pg), and at the top of the mantle (Pn) are clearly identified in the first arrivals; reflected waves from the Moho (P_MP) (Fig. S1) and some reflections from the mid-crustal boundaries are seen in secondary arrivals. Seismometers' horizontal components record converted PS-waves from the basement (PgS) (Fig. S2) and major S phases: Sg, S_MS (Fig. S3). Here and after in this paper, by "pure" S-waves we really consider PS-waves which propagate with transverse polarization along the entire path in the solid medium below the conversion at the seafloor on downgoing raypaths. Large variations in the bathymetry and in the geometry of the acoustic and crystalline basements are the main causes for undulations of the observed arrivals.

Sedimentary *refracted waves* have apparent velocities ranging from 1.8 to 5.4 km/s. Seismic waves with apparent velocities of 3.2–3.5 km/s and higher are the most consistent and are identified only in the first arrivals. Waves with lower apparent velocities are recorded almost for all OBSs only in the secondary arrivals, due to a large water thickness. Most of the sedimentary phases are observed in the first arrivals at offsets of up to 20–25 km.

Different refracted phases are identified by breakpoints in travel-time curves of the first arrivals. However, for fine structural layering with a small velocity contrast the breakpoints are not always visible. Sedimentary S-refractions from the upper part of the sediments are not observed on seismograms, as they have apparent velocities smaller than Vp in water.

Refracted waves associated with the upper crust (Pg) are the best observed along the entire profile. These phases are the first arrivals in the offsets from 15 km to 80 km. The prevailing values of the Pg apparent velocity are 6.2–6.7 km/s. The corresponding S phases (Sg) are identified on the horizontally oriented sensor components (Sg) (Fig.S3). In addition, strong converted phases (PgS) are formed at the top of the crystalline basement. These phases show a constant time shift with respect to Pg (Fig. S2), which indicates that the conversion takes place on the upgoing ray.

Refracted phases coming from the lower crust (PL) become the first arrivals after Pg. They have apparent velocities of 6.7–7.1 km/s and can be identified at offsets of 80–100 km. P_L are usually weaker compared to Pg and have discontinuities in the travel-time curves. S phases refracting in the lower crust are also identified (S_L).

Moho reflections (P_MP) are identified on most OBS records and appear on offsets of 80–100 km (at the eastern part of the profile) and 60–70 km (at the western part). PmP are observed out to 180–200 km offsets, reaching in some cases 220–240 km. The shear-wave Moho reflections (S_MS) are distinctively identified on the horizontal sensor components, but are scattered due to interference of the waveforms (Fig. S3).

The uppermost mantle refractions (Pn) are observed not at all stations. With offsets from 20-30 km to 40–60 km their amplitude varies from very strong to only "guessed" against the background noise. The S refractions (Sn) are observed extremely rarely due to their weakness.

Sub-Moho reflections are present in several OBS records in the central part of the profile. However, due to episodic appearance of these phases, the presence of persistent boundaries in the uppermost mantle is under question.

Fig. S4 (in the Electronic Supplementary Data Section) shows a set of P travel-time curves along the "Arctic-2012" wide-angle profile, which allows identification of different crustal blocks.

(1) The Mendeleev Rise block has a clearly expressed subdivision into the upper and lower crust with a relatively deep Moho.

(2) The Chukchi Basin block is characterized by the Moho uplift, and has a thin and on average high-velocity crust.

(3) The Chukchi Plateau at the eastern end of the profile has a thick low-velocity basement.

(4) The structure of the Vilkitsky Trough block at the western end of the profile is not well resolved (Fig. S4). The interpretations of the MCS data show that the maximum thickness of the sedimentary cover is in the Vilkitsky Trough and in the Chukchi Basin.

3. Combined geophysical model

3.1. Seismic velocity model

Seismic structure along the "Arctic-2012" profile is based on the forward modeling of the travel times for all phases identified in the OBS data (the SeisWide interactive software (Chian and Lebedeva-Ivanova, 2015, Chian et al., 2016) developed by D. Chian based on algorithms and codes of Zelt and Smith (1992)).

3.2. Phases modeling

Stacked MCS reflection section demonstrates a large number of reflecting horizons in the sedimentary cover (see Fig. 2). However, not all of the corresponding reflections are identified from the individual OBS data sections. The velocity-interface model of the sedimentary cover includes only the boundaries identified by the refracted phases (Psed) from the wide-angle data. In addition, secondary refraction arrivals are used when possible (Fig. 3). This way we obtain a robust velocity model comparable with the MCS velocity data. A comparison of velocities calculated from the MCS and OBS data for the location with the greatest sediment thickness shows only minor differences (Fig. 4).

The top of the crystalline basement corresponds to the transition from consistent sub-horizontal reflecting horizons to scattered reflectivity below it, as seen in the MCS section. The velocity contrast

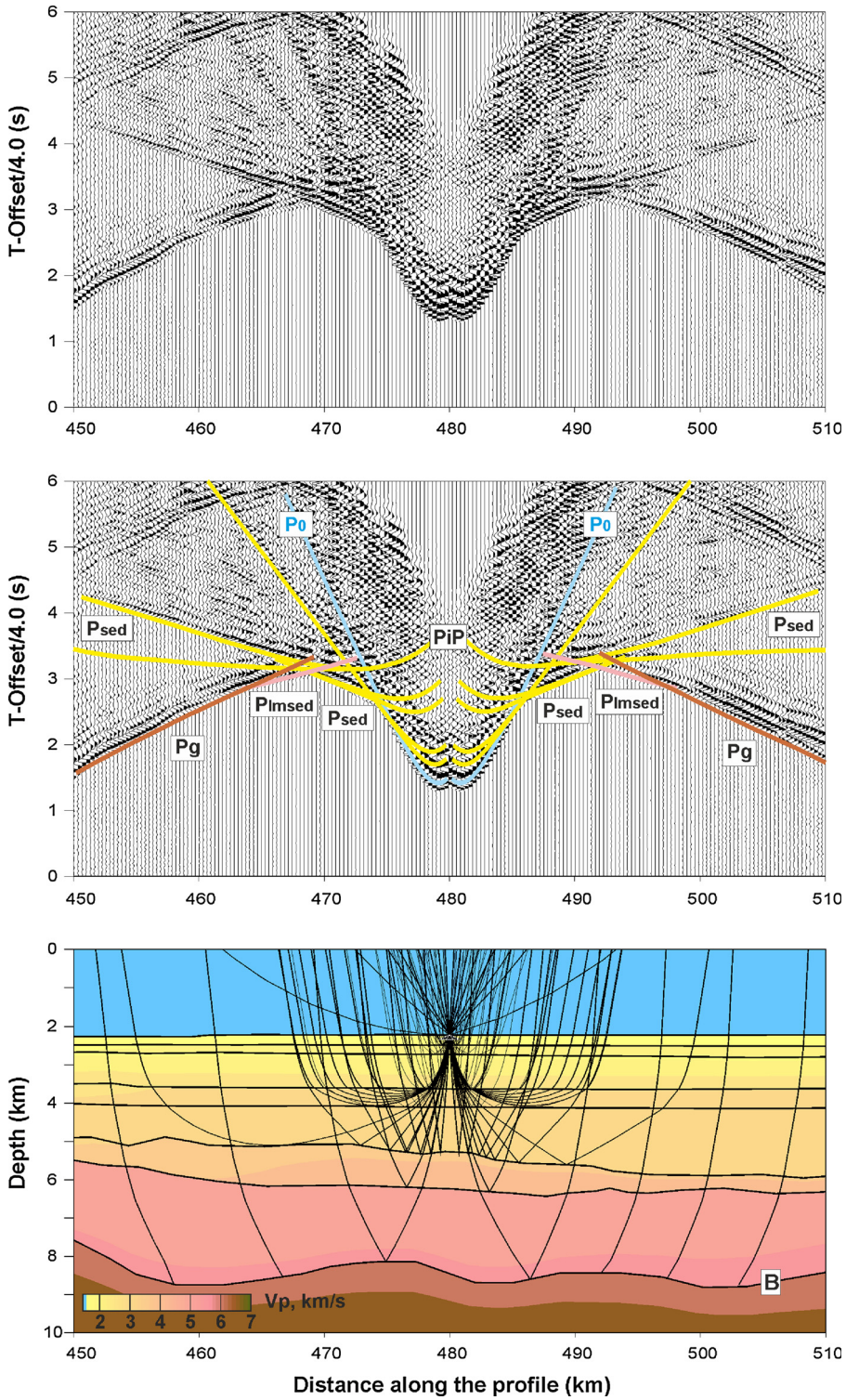

Fig. 3. Example of the data section and ray tracing diagram for refracted and reflected P-waves in the sedimentary cover (OBS 480). P_0–the direct water wave; Psed – refracted waves in the upper sedimentary layer; PiP – mid-sedimentary reflected waves; Plmsed – refracted waves in the lowermost sediments; Pg – refracted waves in the upper crust. B – top of the crystalline basement.

across the top of the crystalline basement is not always sharp. For the major part of the profile, the Vp values at the top of the crystalline basement are in the range of 6.0–6.4 km/s. However, along a large part of the profile the overlying sediments have Vp ~ 4.0–5.6 km/s, locally reaching 6.0 km/s. Such Vp values are intermediate between the values typical for sediments and for the crystalline basement, with similar observations reported earlier in the Arctic Ocean (Lebedeva-Ivanova et al., 2006; Poselov et al., 2011; Funck et al., 2011). We interpret this layer as corresponding to (meta)sedimentary rocks. Refracted waves from this layer (Plmsed) are identified in the first arrivals (see Fig. S5 in the Electronic Supplementary Data Section).

Examples of the crustal (crystalline basement) refractions (Pg, P_L), Moho reflections (P_MP), and refracted mantle phases (Pn) are shown in Fig. 5. Vp in the upper/middle crust is 6.0–6.7 km/s, increases in the

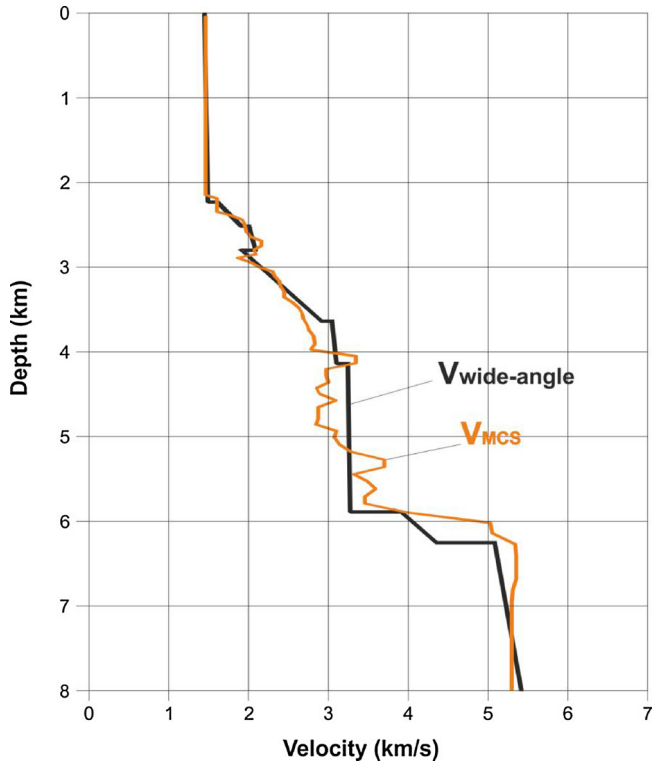

Fig. 4. Comparison of Vp velocity vertical profile obtained from the MCS and wide-angle data at the OBS 480 location for the shallow part of the profile.

lower crust to 6.8–7.3 km/s, and reaches 7.8–8.0 km/s in the uppermost mantle.

3.3. PS-wave modeling

The best recorded converted waves are registered on the horizontal radial component and correspond to PgS-waves. The conversion takes place at the top of the crystalline basement on the upgoing raypaths. Raytracing modeling of these phases is done by specifying the conversion boundary and the Poisson's ratio (or the Vp/Vs ratio). An example of PgS modeling is given in Fig. 6. Calculations show that Vp/Vs in the sediments varies from 1.9 to 2.8 with an average of 2.3. For the lowermost sedimentary layer (interpreted as metasediments), the estimate of Vp/Vs is around 2.0.

3.4. S-wave modeling

On average, along the "Arctic-2012" profile, it was possible to identify S-wave Moho reflections (SmS) for half of the stations and some S refraction phase for one third of the instruments. Examples of modeled refracted S-waves (Sg, S_L) in the crystalline basement and Moho reflections (S_MS) are shown in Fig. 7. The estimate of Vp/Vs is 1.70–1.78 in the crystalline basement, in sharp contrast to high values in the sedimentary sequences.

3.5. Assessment of picking errors and the velocity model uncertainties

The crustal and upper mantle velocity model along the "Arctic-2012" profile is based on modeling of P-, S-, and converted waves (Fig. 8). We use the Rayinvr software package (Zelt and Smith, 1992) to evaluate the uncertainties of the model.

It is commonly accepted that model quality is fine if the root-mean-square (RMS) error does not exceed 50–100 ms for P travel times and 100–200 ms for S and converted waves travel times, while the normalized value of χ^2 does not exceed 1. In this case, the velocity uncertainties are expected to be ± 0.1–0.2 km/s. Table 1 shows RMS misfit and χ^2 criterion for all types of phases used in the raypath modeling.

The analysis of the travel-time data (Table 1) shows that the RMS values are reasonable for all P- and PS-phases. The RMS values for S phases (especially for Sg) slightly exceed the picking uncertainty of 200 ms.

The examples of the raytracing are shown in Figs. 9–11. High raypaths density for P phases in the crust and uppermost mantle is sufficient for reliable velocity modeling (Fig. 9). The shallow structure is resolved also by the converted PS-waves (Fig. 10). S phases have been identified only fragmentarily, limiting the number of the travel-time picks (Fig. 11). Therefore, it is possible to use S phases only for a rough estimate of Vp/Vs, but not for a detailed vs model.

3.6. Modeling of gravity anomalies

We test the final velocity model by calculating a 2D density model along the "Arctic-2012" profile to fit the observed gravity field (see Fig. 1; Gaina et al., 2011). The initial density model is constrained by seismic velocities converted to density values:

$\rho = 0.23Vp^{.25}$ for sediments (Gardner et al., 1974),

$\rho = 0.18Vp + 0.4\ (Vp/Vs) + 1.02$ for the basement (Kashubin, 1984).

The average in situ density of the uppermost mantle is assumed to be 3.35 g/cm^3 (Krasovsky, 1981), which corresponds to sub-Moho temperatures of 350–420 °C assuming mantle peridotite density of 3.39–3.40 g/cm^3 at room conditions. For the estimated Moho depth of 25–35 km along the profile, such sub-Moho temperatures may all be fit by a 60–65 mW/m^3 continental geotherm (Pollack and Chapman, 1977).

Forward gravity modeling for density values based on the above specified Vp-density conversion shows a significant misfit between the observed and the calculated gravity fields. Therefore, the initial density model is corrected based on a 3D solution of the inverse gravity problem in the spectral domain (Milshtein et al., 2008). As *a priori* information, we use the depth to the major seismic interfaces and the velocity variations with depth. The density model is iteratively adjusted until an acceptable fit to the gravity field is achieved. The final density model along the "Arctic-2012" profile is shown in Fig. 12. The model fits the observed gravity field with the RMS error of 4 mGal and with the maximum misfit of < 10 mGal.

The density values increase with depth from 2.00 to 2.50 g/cm^3 in the upper sedimentary layer to 2.50–2.67 g/cm^3 in the lower sedimentary layer (metasediments), to 2.60–2.83 g/cm^3 in the upper/middle crust, and to 2.85–3.01 g/cm^3 in the lower crust. Below the Mendeleev Rise, the lower crustal density reaches 3.10 g/cm^3. Density of the uppermost mantle varies from 3.27 g/cm^3 below the Chukchi Basin to 3.40 g/cm^3 at a 38–40 km depth below the Mendeleev Rise.

4. Results: structure of the crust and uppermost mantle

Our final seismic velocity and density models along the "Arctic-2012" wide-angle profile are shown in Figs. 8 and 12, respectively. We discuss below the structure and a possible nature of different layers from top to bottom.

4.1. Sedimentary layer

The upper *sedimentary layer* is clearly identified from low-angle bedding of reflectors in the MCS section (see Fig. 2). Its thickness reaches 7–8 km in the Vilkitsky Trough, 4 km in the Chukchi Basin, and decreases to 0.5–1.0 km in the Mendeleev Rise. P-wave velocities increase with depth from 1.6–1.9 km/s in the upper part of the layer to 4.8–5.6 km/s at its bottom in the deepest parts. The Vp/Vs ratio varies widely from 1.9 to 2.8. Densities, as a rule, do not exceed 2.4–2.5 g/

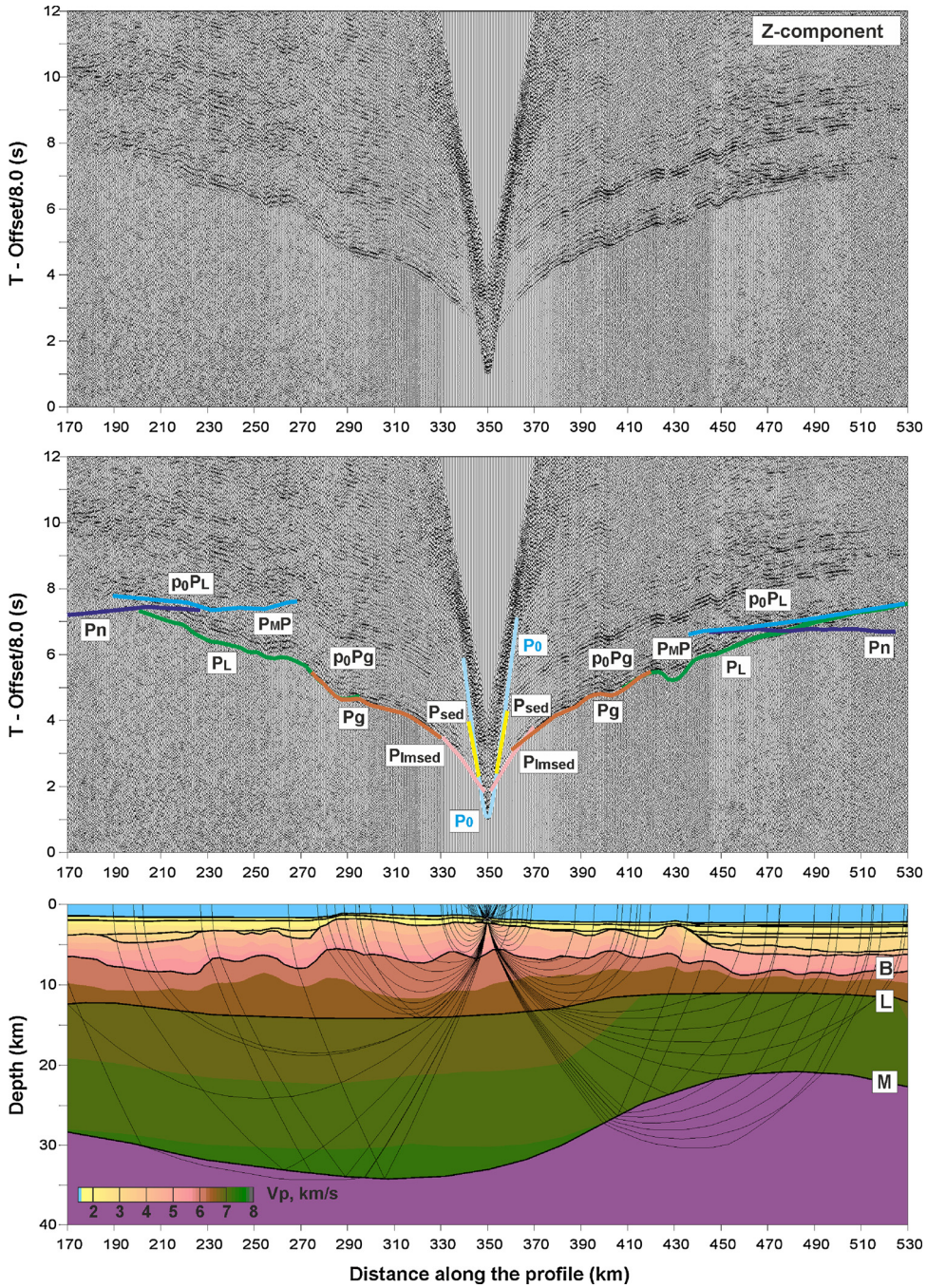

Fig. 5. Example of the data section and ray tracing diagram for refracted and reflected P-waves in the crust and uppermost mantle (OBS 350). Pg – refracted waves in the upper crust; P_L – refracted waves in the lower crust; p_0Pg, p_0P_L – refracted waves in the upper and in the lower crust after reverberation in the water layer; P_MP – Moho reflection; Pn – refracted waves in the uppermost mantle; other abbreviations are as on Fig. 3. Thick lines show major seismic boundaries: B – top of the crystalline basement, L – top of the lower crust, M – Moho.

cm^3. The results are consistent with geological sampling of the sedimentary cover on the Mendeleev Rise which revealed that it is composed of quartz and feldspar-quartz sandstones, dolomite and limestone (Morozov et al., 2013).

The *lowermost sedimentary (possibly metasedimentary) layer* is present not in all parts of the profile. Its presence is identified from the transition from regular subhorizontal reflections to irregular inclined reflectors in the MCS section. The layer is identified in the Mendeleev Rise with a thickness of up to 3–5 km, the thinner sequence (1.5–2.0 km) is present in the Chukchi Basin and the layer may be locally present within the Chukchi Plateau. However, the layer has not been identified in the Vilkitsky Trough.

The lowermost sedimentary layer has Vp values (4.0–6.0 km/s) intermediate between sediments and the basement and the Vp/Vs ratio of 1.9–2.0. We note that a sedimentary layer with similar Vp (5.0 km/s and higher) has been observed off-shore mid-Norway where, based on seismic and drilling data, it has been interpreted as the post-Cretaceous sediments (Mjelde et al., 1996). In the Arctic Ocean, greenschist, metabasite, and gneiss have been dredged in the escarpments of the Mendeleev Rise; two deep-sea drilling wells in the northern and southern parts of the Mendeleev Rise recovered the core of Cretaceous cenotype basalts (trachybasalt and trachyandesite) (Morozov et al., 2013), which apparently belong to the High-Arctic Large Igneous Province (Gottlieb et al., 2010). We therefore interpret the lowermost

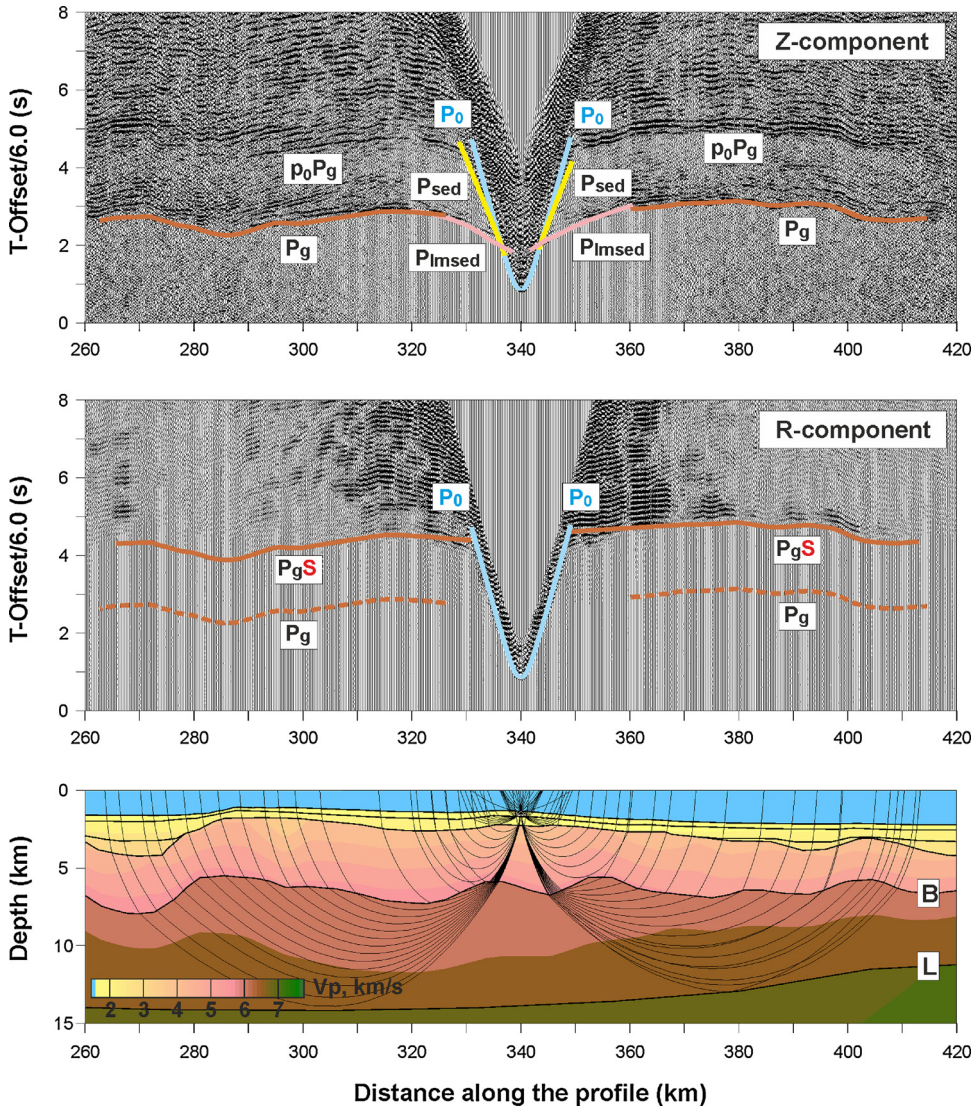

Fig. 6. Example of the data section and ray tracing diagram for refracted P-waves in the upper crust and converted PgS-waves (OBS 340). PgS – refracted waves PS-converted at the top of the crystalline basement on the upgoing raypath after P-wave refraction in the upper crust. Other abbreviations are as on Fig. 3, 5.

sedimentary layer as a metasedimentary layer with the presence of volcanic rocks, despite strong reflections indicative of sill intrusions are not observed in our high quality MCS data.

4.2. Crystalline basement

The upper part of the crystalline basement (the upper and middle crust) is determined from Vp and it has Vp ~ 6.0–6.4 km/s at the top of the layer (the uppermost upper crust) and Vp ~ 6.7–6.8 km/s at the bottom of the layer (the lowermost middle crust). The layer has relatively low Vp/Vs values (1.70–1.73) typical of the continental crust (Fig. 8). The average densities of rocks composing the upper/middle crust vary from 2.69 to 2.83 g/cm^3. However, several lenses (20–50 km across and 5–10 km thick) with a low-density material (2.60–2.67 g/cm^3) are recognized at 5–12 km depth in the upper crust of the Chukchi Plateau. The eastern part of the Chukchi Plateau apparently lacks the upper crust with Vp ~ 6.0–6.4 km/s, while this layer is clearly present along all other parts of the "Arctic-2012" profile (Fig. 8).

The thickness of the upper/middle crustal layer varies from 15 to 18 km under the Chukchi Plateau to 3 km under the Chukchi Basin. In the Mendeleev Rise, the thickness of the upper crust is 7–8 km. The composition of the upper crust is not known from geological sampling, but it can consist of volcanic and metamorphic rocks of mainly felsic to intermediate composition (Aleinikov et al., 1991; Christensen, 1996). This conclusion is supported by the presence of granite, gneiss granite, granodiorite and gabbro-dolerite fragments in samples dredged at the Mendeleev Rise (Morozov et al., 2013; Petrov et al., 2016).

The lower crust is characterized by Vp of 6.8–7.3 km/s, the Vp/Vs ratio of 1.74–1.78, and an average density of 2.85–3.01 g/cm^3. Its thickness is surprisingly uniform along the entire "Arctic-2012" profile, ranging from 9 to 12 km beneath the Vilkitsky Trough, the Chukchi Basin and the Chukchi Plateau and increasing to ca. 20 km beneath the Mendeleev Rise (Figs. 8, 12) where it includes a 3–4 km thick high-velocity lowermost crust.

The high-velocity lowermost crust with a high Vp (7.3 km/s) and high-density (3.10 g/cm^3) is recognized only under the Mendeleev Rise and we interpret this layer as magmatic underplaying (Thybo and Artemieva, 2013) related to intraplate mafic volcanism and the HALIP formation.

The crustal thickness ranges from ca. 18–23 km beneath the Chukchi Basin and the Vilkitsky Trough to ca. 28–29 km beneath the Chukchi Plateau and 33–34 km beneath the Mendeleev Rise. The thickness of the crystalline basement is ca. 14–15 km in the Vilkitsky Trough, ca. 12 km in the Chukchi Basin, 25–27 km in the Chukchi Plateau, and 26–29 km

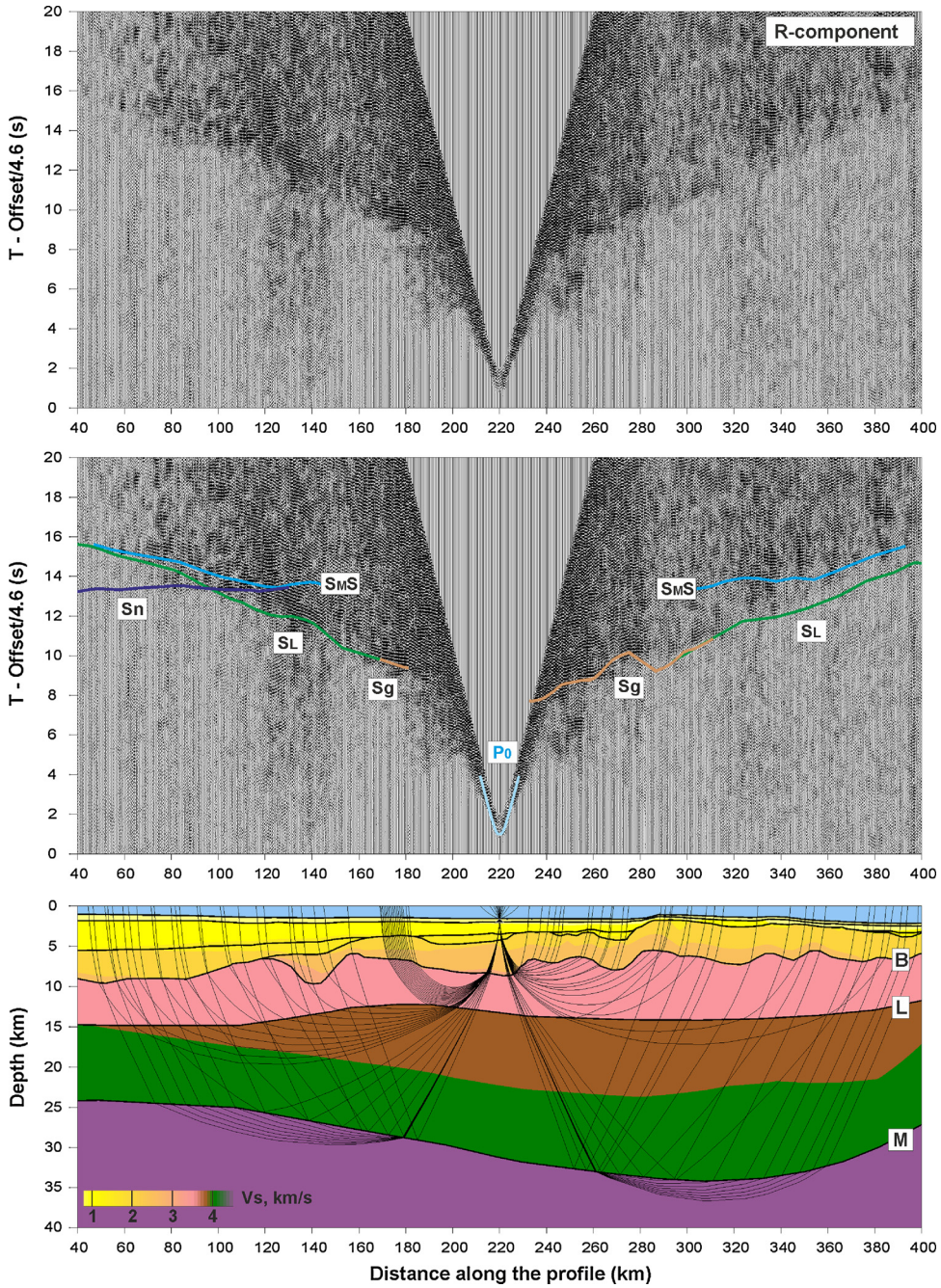

Fig. 7. Example of the data section and ray tracing diagram for refracted and reflected S-waves from the crust and uppermost mantle (OBS 220). Sg – refracted waves from the upper/middle crust; S_L – refracted waves from the lower crust; S_MS – reflected waves from the Moho; Sn – refracted waves in the uppermost mantle; B – top of the crystalline basement (upper crust); L – top of the lower crust; M – the Moho boundary.

beneath the Mendeleev Rise.

4.3. Upper mantle

The uppermost mantle is characterized by normal Vp values of 7.8–8.0 km/s. The average density in the uppermost mantle is ca. 3.35 g/cm^3. However, the region with the most shallow Moho under the Chukchi Basin has the uppermost mantle density (at a 22–27 km depth) as low as 3.27 g/cm^3, while below the deepest Moho under the Mendeleev Rise it may reach 3.40 g/cm^3 at a 35–40 km depth (see Fig. 12). We discuss a possible geodynamic origin of these anomalies in the next section.

5. Discussion

5.1. Origin of the density anomalies

Density anomalies may be caused either by differences in temperature or in chemical composition, or both. A density drop by ca. 0.08 g/cm^3 in the sub-Moho upper mantle beneath the Chukchi Basin, as compared to the "normal" mantle in the adjacent parts of the profile (Fig. 12), requires a ca. 700 °C temperature anomaly, if all density decrease is of thermal origin only (for thermal expansion coefficient of 3.5×10^{-5} 1/K and "normal" mantle density of 3.35 g/cm^3). Such huge temperature anomaly is not possible even when a region is affected by a mantle plume, and the density anomaly clearly indicates the

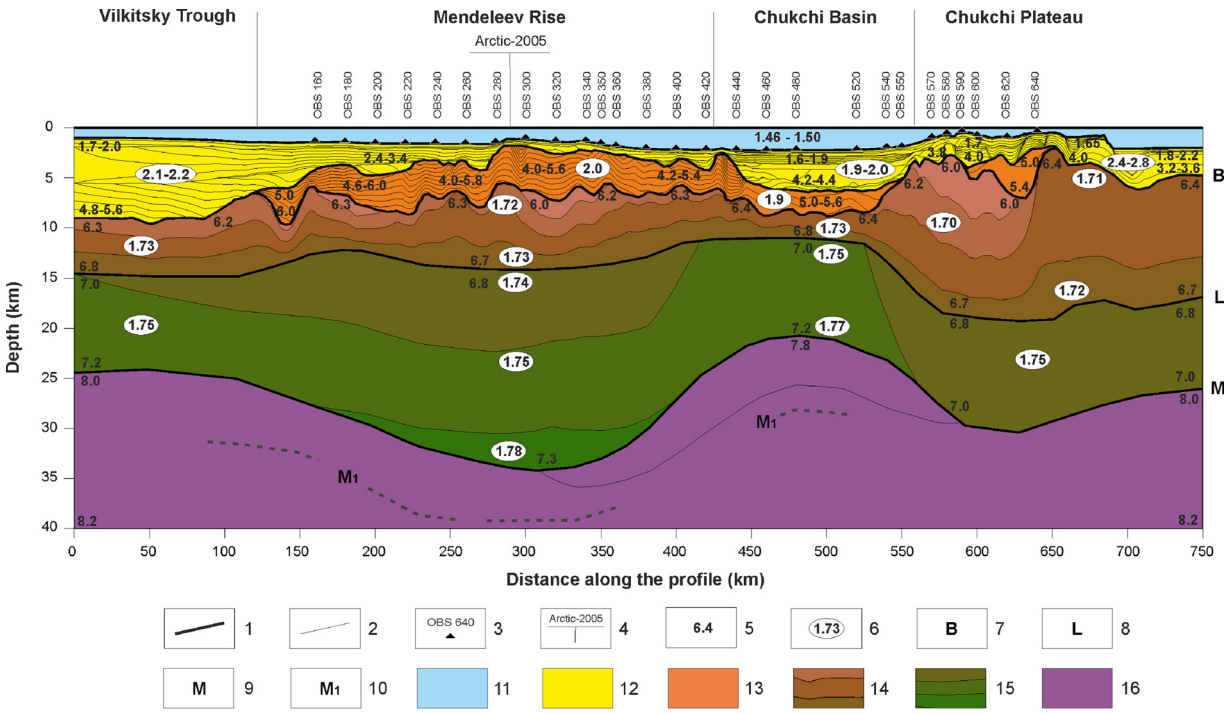

Fig. 8. Final seismic velocity model along the "Arctic-2012" profile. 1–major crustal seismic boundaries; 2–Vp isolines with an interval of 0.2 km/s; 3–OBS positions; 4–intersection with the Arctic-2005 profile; 5–Vp values (km/s); 6–Vp/Vs ratio; 7–top of the crystalline basement; 8–top of the lower crust; 9–the Moho; 10–sub-Moho interface; 11–water; 12–the upper sedimentary layer; 13–the lowermost sedimentary (metasedimentary) layer; 14–the upper/middle crust; 15–the lower crust; 16–the uppermost mantle.

Table 1
Picking errors and raytracing uncertainties for all seismic phases used in the modeling.

Phase	Assumed picking uncertainty (ms)	Number travel times	RMS error (ms)	χ^2
P_0	50	685	21	0.174
Psed	50	703	36	0.530
Plmsed	50	1426	45	0.801
Pg	100	7885	87	0.752
P_L	100	8864	111	1.222
P_MP	100	10672	75	0.556
Pn	100	1514	73	0.537
$P_{M1}P$	100	1534	50	0.248
PgS	100	5827	63	0.426
P_LS	100	1475	57	0.392
Sg	200	152	293	2.154
S_L	200	316	212	1.126
S_MS	200	307	208	1.090
Sn	200	47	124	0.395

presence of a strong compositional anomaly in the upper mantle of the Chukchi Basin. Furthermore, a recent high-resolution seismic tomography model for the Arctic Ocean (Lebedev et al., 2017) does not show any significant shear-velocity anomaly beneath the Mendeleev Rise-Chukchi Basin region at shallow depths (< 100 km), while it shows a strong low-velocity anomaly (ca. 6%) beneath this region centered at around 200 km depth. The lateral size of the anomaly is significantly larger than the Chukchi Basin and its origin is speculative.

We note that the crystalline crust beneath the Chukchi Basin is thinned to 12 km only (Fig. 12). We speculate that a hyperextension of the crust with a possible formation of crustal-scale fractures may have allowed seawater to penetrate through the crust and to serpentinize the upper mantle peridotites. For serpentinite density of 2.6–2.7 g/cm^3, the mantle density anomaly beneath the Chukchi Basin requires ca. 10% serpentinization at a 22–27 km depth and ca. 5% serpentinization at a 27–35 km depth, in case all density anomaly is caused by this metamorphic reaction. The reduced upper mantle Vp velocity (7.8 km/s versus 8.0 km/s) beneath the Chukchi Basin can also be explained by the same degree of serpentinization of mantle peridotite (for serpentine Vp ~ 5.8 km/s, Courtier et al., 2004).

The penetration of seawater through the crust would have also caused phase transitions in the lower crustal material to garnet granulite (density 3.0–3.2 g/cm^3) or even partial eclogitization of the lower crust. In the latter case, the high-density (3.01 g/cm^3), high-velocity (7.2 km/s) lower crustal anomaly beneath the Chukchi Basin may be explained by the presence of ca. 20% of eclogitic material in the lower part of the lower crust (assuming "normal" lower crustal density of 2.90 g/cm^3 and eclogite density of 3.46 g/cm^3 (Ito and Kennedy, 1971; Austrheim, 1987)).

We note that the Vilkitsky Trough also has a thin crust (with a 14–15 km thick crystalline basement) and a high-density (3.01 g/cm^3), high-velocity (7.2 km/s) lower part of the lower crust, and therefore it may have been affected by the same metamorphic processes as the Chukchi Basin. However, the absence of density anomalies in the upper mantle suggests that seawater did not penetrate the Moho at the Vilkitsky Trough.

Similar to the Chukchi Basin, a 3–4 km thick high-density (3.1 g/cm^3), high-velocity (7.3 km/s) underplated material in the thick lower crust of the Mendeleev Rise may be made of garnet granulite or a partially eclogitized basaltic underplate, while the presence of eclogites in the upper mantle lithosphere is suggested by a high density anomaly below a 35 km depth. It is hardly possible to put any age constraints on these metamorphic processes, and the upper mantle density anomaly can be an old (Precambrian/early Paleozoic) eclogite body.

The lower crust of the Chukchi Plateau has only minor density anomaly in the lower part of the crust, however it has low-density bodies in the upper crust (2.60–2.67 g/cm^3). We note that the Chukchi Plateau also has an increased thickness of the upper crust (ca. 16 km as compared to 3–8 km in other parts of the profile) and propose that the low-density upper crustal bodies may be associated with magmatic intrusions.

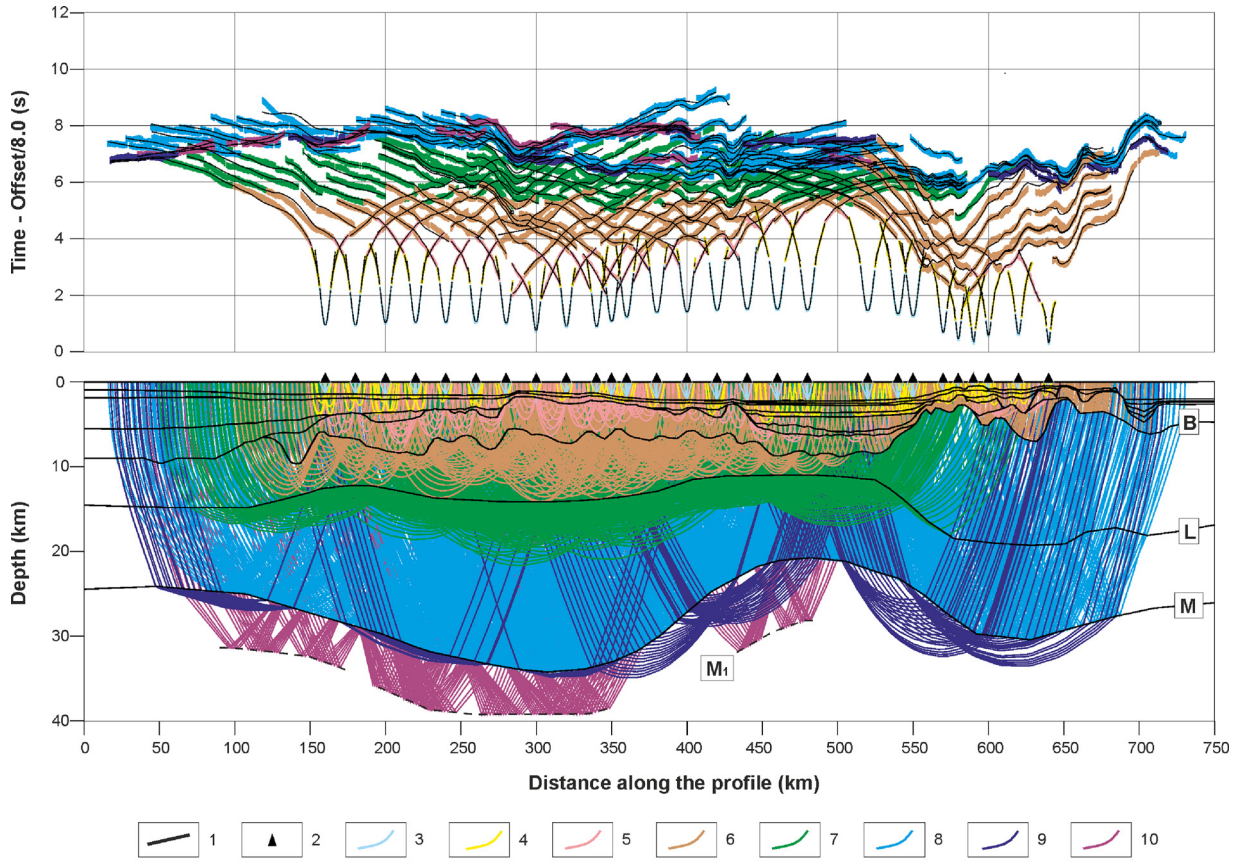

Fig. 9. Observed and calculated P travel-times (upper panel) and calculated raypaths (lower panel) for the Vp velocity model. Every tenth modeled raypath is plotted for clarity. 1–seismic interfaces; 2–projections of the OBS positions to the sea-surface; 3–direct water wave (P_0); 4–refracted waves from the upper sedimentary layer (Psed); 5–refracted waves from the lowermost sedimentary (metasedimentary) layer (Plmsed); 6–refracted waves from the upper/middle crust (Pg); 7–refracted waves in the lower crust (P_L); 8–Moho reflections (P_MP); 9–refracted waves in the uppermost mantle (Pn); 10–reflections from the sub-Moho boundary ($P_{M1}P$). Observed travel times are shown by the corresponding color bars; the calculated travel-time curves are shown by black lines. The size of bars representing picked travel times corresponds to the value of the assumed uncertainty. Symbols for the interfaces are the same as in Fig. 8.

5.2. Tectonic nature of the crust

On the whole, by the Vp and Vp/Vs structure, the crust along the entire "Arctic-2012" profile corresponds to the continental type. The presence of the upper/middle crust, presumably of felsic-intermediate composition, and the Vp/Vs ratio in the basement typical of the continental crust (1.70–1.78, in contrast to values typical of the oceanic crust of 1.81–1.87 (Hyndman, 1979)) provides a strong support for its continental origin (Kashubin et al., 2013). This conclusion is in agreement with recent studies which argue for a continental origin of the Alpha-Mendeleev system of bathymetry highs (Oakey and Saltus, 2016).

5.3. Comparison with other studies

The Alpha-Mendeleev Rise System has been studied in recent years by several wide-angle profiles (Fig. 1), which resulted in a number of crustal and uppermost mantle Vp models (Fig. 13). There is a general agreement between the velocity models for the Mendeleev Rise, despite different seismic profiles crossed different parts of the bathymetry high.

All interpretations recognize high-Vp sedimentary (metasedimentary) sequences, the upper and lower parts of the crust, with similar Vp velocities and thicknesses of the individual layers in different models. The presence of the crust-mantle layer (underplated material?) with Vp velocities of 7.4–7.6 km/s was identified along the "Arctic-2000" profile (Lebedeva-Ivanova et al., 2006). Along the "Arctic-2005" profile, the Vp values in the lower crust immediately above the Moho are significantly lower than in other profiles (6.9 km/s in contrast to 7.3 km/s) (Poselov et al., 2011). However, these differences do not affect the generally consistent interpretation of the crustal structure of the Mendeleev Rise and demonstrate a remarkable similarity of its deep structure with the crustal structure of the Alpha Ridge (Fig. 13).

A comparison of the Vp model for the crust and uppermost mantle of the Mendeleev Rise with velocity models for the Iceland-Faroe Ridge and the Kerguelen Plateau shows a significant similarity (Fig. 14). The Iceland-Faroe Ridge and the Kerguelen Plateau are chosen for comparison because it has long been proposed that both of these oceanic structures were formed as a result of extensive volcanic activity – on the oceanic crust in case of the Iceland-Faroe Ridge (Bohnhoff and Makris, 2004, etc.) and on the continental crust in case of the Kerguelen plateau (Operto and Chavis, 1995, etc.). Gravity and magnetic data were used recently (Oakey and Saltus, 2016) to argue that the closest analogue for the Alpha-Mendeleev system is the continental part of the Kerguelen plateau. Our results support this conclusion on the continental nature of the crust at the Mendeleev Rise and its significant magmatic overprint.

A comparison of velocity models for the crust and the uppermost mantle of the Mendeleev Rise, the Iceland-Faroe Ridge and the Kerguelen Plateau (Fig. 14) clearly shows their similarity, with the most pronounced differences in the upper 10 km, which corresponds to the difference between the felsic upper continental crust in the Mendeleev Rise and the Kerguelen Plateau and the mafic oceanic crust in the Iceland-Faroe Ridge. As noted above, the Vp/Vs values modeled for the Mendeleev Rise from multicomponent observations indicate the felsic-intermediate composition of the upper/middle crust, and its continental

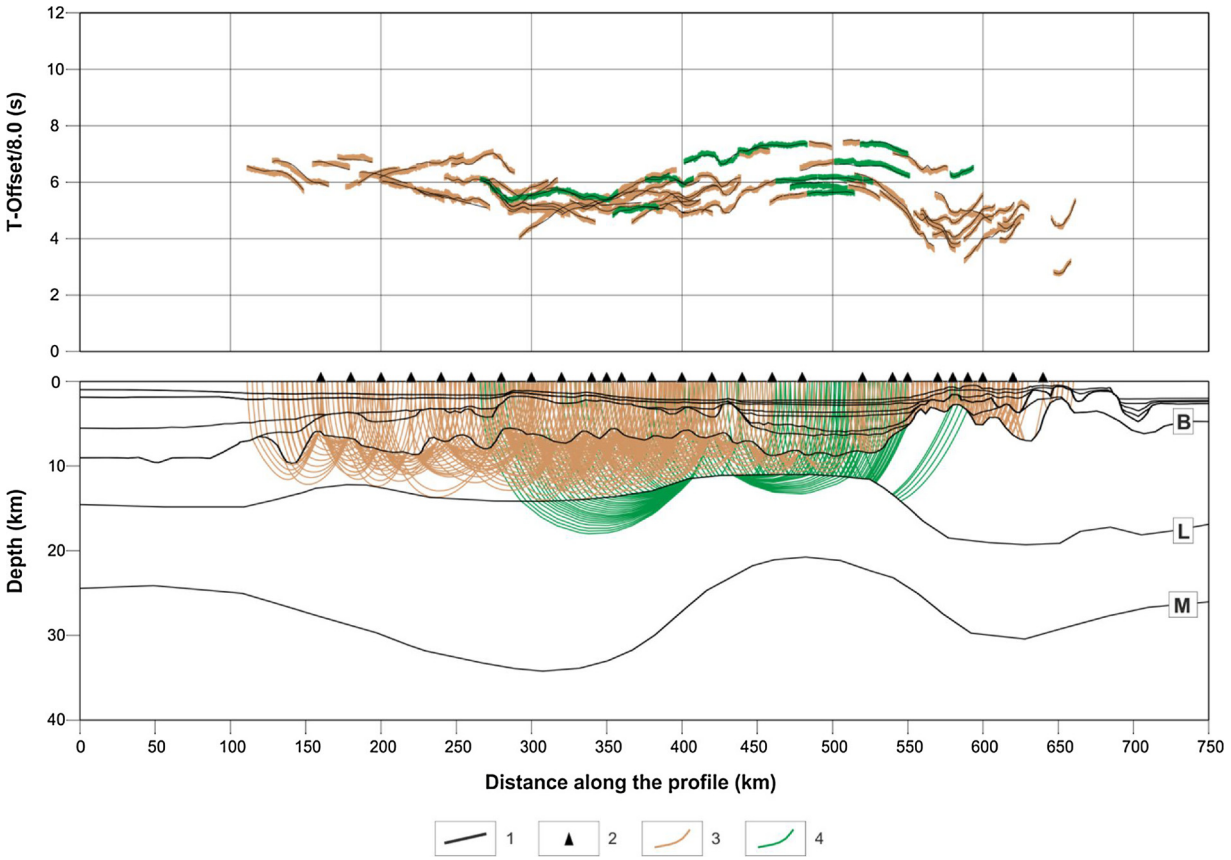

Fig. 10. Observed and calculated converted PS travel-times (upper panel) and calculated raypaths (lower panel). Every tenth modeled raypath is plotted for clarity. 1–seismic interfaces; 2–the OBS positions; 3–PgS; 4–P_LS. Further details are as in Fig. 9.

nature is further supported by the results of isotope-geochemical studies of the bottom-rock material sampled in the Mendeleev Rise escarpments (Morozov et al., 2013).

6. Conclusions

We report interpretation of wide-angle reflection and refraction data which were acquired, for the first time, in the high-latitude Arctic Ocean across the Mendeleev Rise at 77°N. A dense array of ocean bottom seismometers with a 3-component recording of the wave field allowed for detailed interpretation of the crustal and upper mantle structure down to ca. 40 km depth. The MCS seismic data along the same 740 km long profile allowed to model a detailed structure of the sedimentary cover and the uppermost crystalline crust. Joint interpretation of seismic and gravity data allowed for determining Vp, Vp/Vs and density in the crustal layers and the uppermost mantle.

1. We observe a strong variability in the crustal structure beneath the northeastern Vilkitsky Trough, the Mendeleev Rise, the Chukchi Basin, and the Chukchi Plateau, with the Moho depth ranging from ca. 24 km in the Vilkitsky Trough and ca. 21 km the Chukchi Basin, to ca. 30 km in the Chukchi Plateau, and to ca. 33–34 km beneath the Mendeleev Rise. The thickness of the crystalline basement ranges from ca. 14–15 km in the Vilkitsky Trough and ca. 12 km in the Chukchi Basin, to 25–27 km in the Chukchi Plateau, and to ca. 26–29 km beneath the Mendeleev Rise.
2. The sedimentary cover, including both the upper layer of sediments (typically with Vp < 4.5 km/s) and the lowermost sedimentary layer with Vp > 4.0 km/s, varies in thickness from ca. 8 km in the Vilkitsky Trough, to 6 km (including 4 km of the upper sedimentary layer) in the Chukchi Basin, 2–4 km in the Chukchi Plateau (with a 2–3 km thick upper layer of sediments), and 3–7 km (including less than 1 km thick upper layer of sediments) in the Mendeleev Rise.
3. The upper/middle crust with seismic characteristics of felsic-intermediate continental upper crust (Vp ~ 6.0–6.8 km/s and Vp/Vs ~ 1.70–1.73) is present along the entire profile. The thickness of this crustal layer is 6–8 km along the profile, except for the Chukchi basin where it thins to 3–4 km and the Chukchi Plateau where its thickness increases to 15–18 km with the presence of low-density (2.60–2.67 g/cm^3) upper crustal bodies, interpreted as magmatic intrusions.
4. The lower crust (Vp ~ 6.8–7.3 km/s and Vp/Vs ~ 1.74–1.78) is the most uniform in thickness (ca. 10 km), except for the Mendeleev Rise where this layer is ca. 20 km thick. A 3–4 km thick high-Vp (Vp ~ 7.3 km/s and Vp/Vs ~ 1.78), high density (3.10 g/cm^3) lower part of the lower crustal layer is present only below the Mendeleev Rise and we interpret it as underplated magmatic material, while the high density upper mantle anomaly (3.40 g/cm^3 at depths > 35 km) is interpreted as an eclogitic body.
5. The sub-Moho upper mantle Vp velocities are ca. 8.0 km/s beneath the Vilkitsky Trough and the Chukchi Plateau, and reduce to 7.8 km/s beneath the Chukchi Basin. The presence of a high-density (3.01 g/cm^3) body in the lower part of the lower crust, necking of the crystalline crust to ca. 12 km in thickness, and the presence of a low-velocity (7.8 km/s), low-density (3.27–3.31 g/cm^3) upper mantle body beneath the Chukchi Basin suggest basalt to garnet granulite phase transitions (with a possible particle eclogitization) in the lower crust and 5–10% serpentinization of the upper mantle at a 22–35 km depth, possibly caused by seawater penetration through the crust to the uppermost mantle during crustal hyperextension.
6. We recognize a discontinuous seismic reflector 6–7 km below the

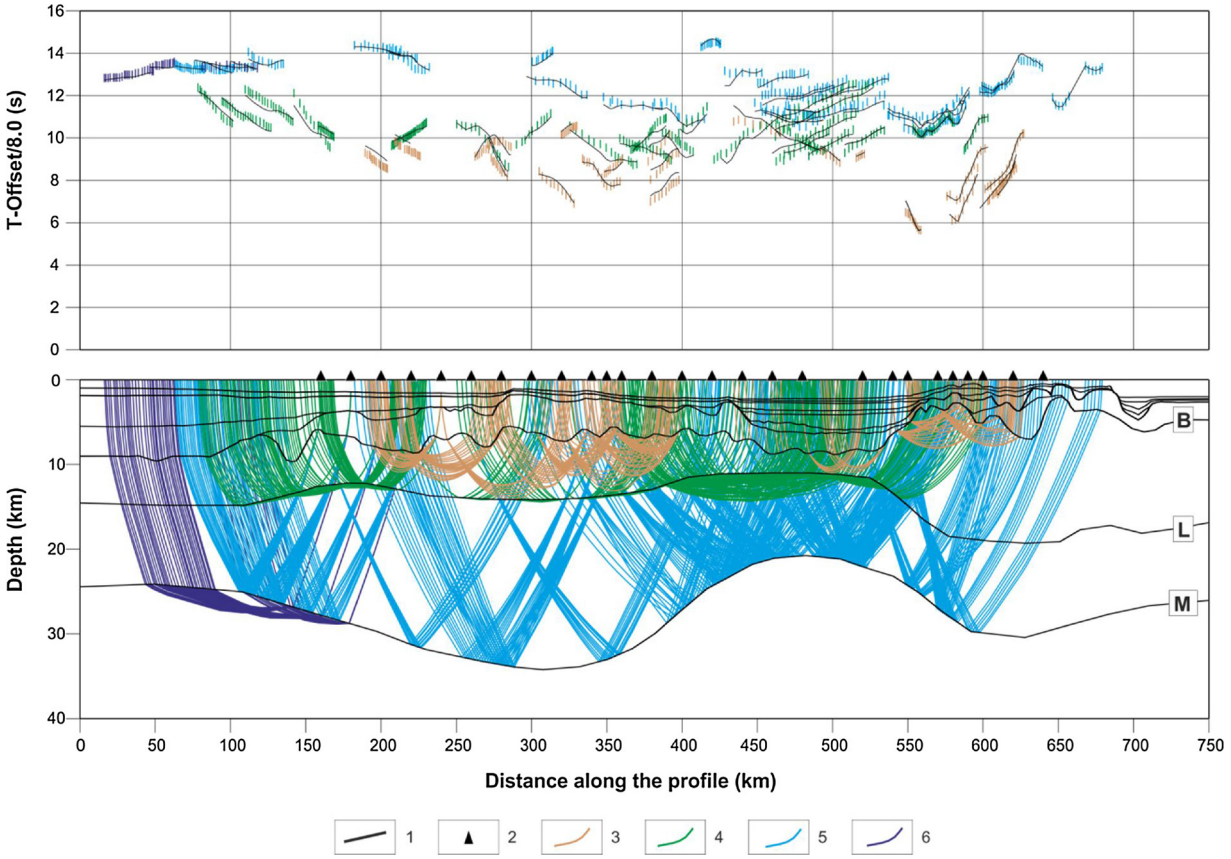

Fig. 11. Observed and calculated S travel-times (upper panel) and calculated raypaths (lower panel) for the vs velocity model. Each modeled raypath is plotted. 1–seismic interfaces; 2–the OBS positions; 3–refracted waves in the upper/middle crust (Sg); 4–refracted waves in the lower crust (S_L); 5–Moho reflections (S_MS); 6–refracted waves in the uppermost mantle (Sn). For further explanations see Fig. 9.

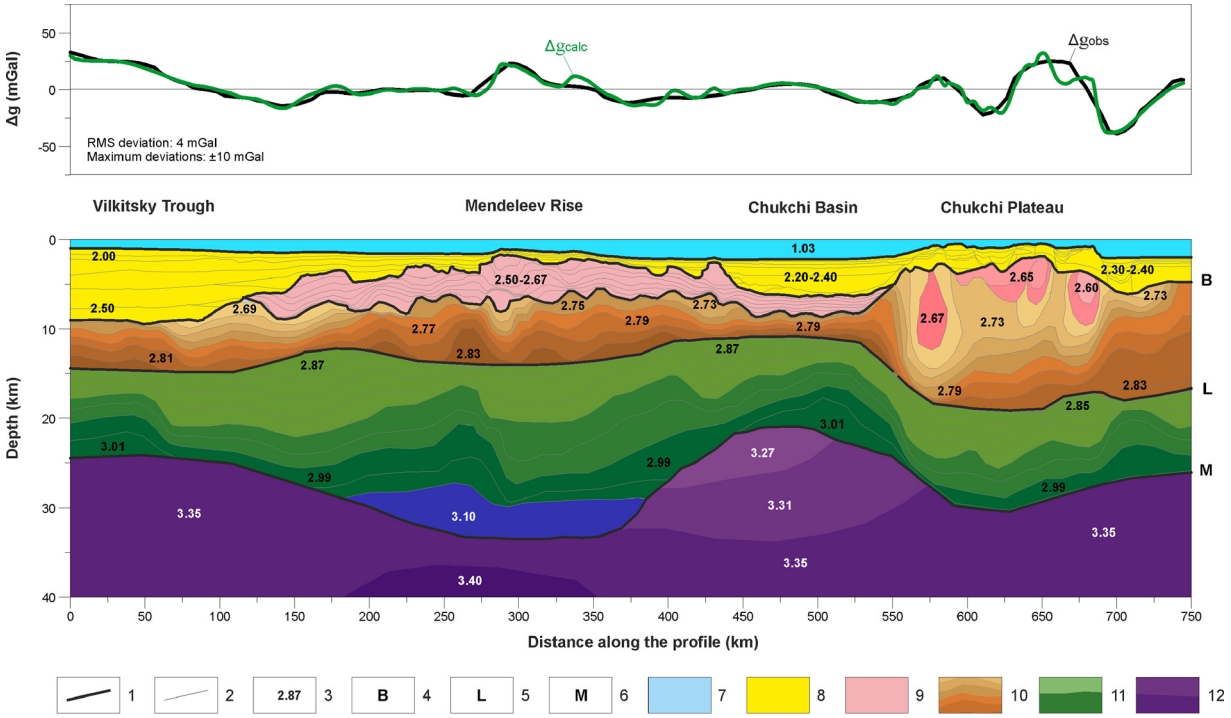

Fig. 12. Crustal and uppermost mantle density model along the "Arctic-2012" profile. 1–main density boundaries in the crust; 2–main density boundaries in the sedimentary cover and density contours with an interval of 0.02 g/cm^3 in the basement; 3–density values in g/cm^3; 4–top of the crystalline basement; 5–top of the lower crust; 6–Moho; 7–water; 8–the upper sedimentary layer; 9–the lowermost sedimentary (metasedimentary) layer; 10–the upper/middle crust; 11–the lower crust; 12–the uppermost mantle.

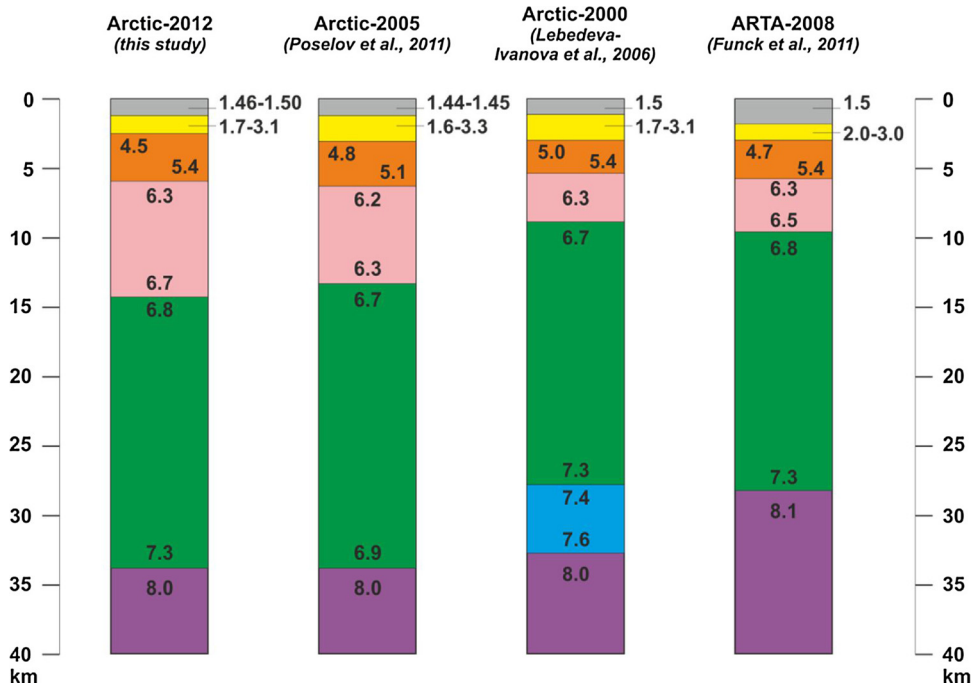

Fig. 13. Comparison of the crustal and uppermost mantle Vp velocity model along the "Arctic-2012" profile with other velocity models for the Mendeleev Rise and Alpha Ridge (numbers – velocity values in km/s, seismic profile locations are shown in Fig. 1).

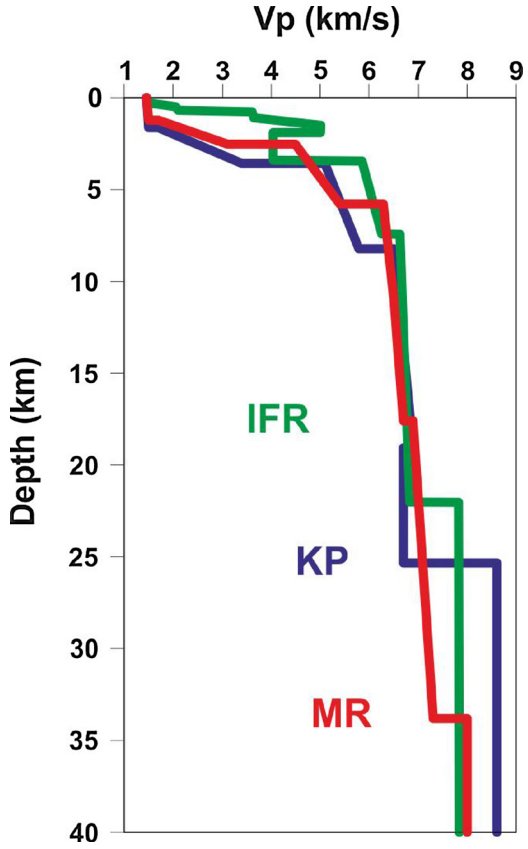

Fig. 14. Comparison of the crust and the uppermost mantle P-wave velocity depth profile for the Mendeleev Rise (MR) (this study), the Iceland-Faroe Ridge (IFR) (Bohnhoff and Makris, 2004) and the Kerguelen Plateau (KP) (Operto and Charvis, 1995).

Moho (at 30 km below the Vilkitsky Trough and the Chukchi Basin and at ca. 40 km depth beneath the Mendeleev Rise).

7. Our results support the continental nature of the crust along the entire profile and suggest that the Alpha-Mendeleev system of bathymetry highs was formed on the continental crust by mafic magmatism, probably related to the HALIP, as supported by independent geological, geochemical and geophysical studies of the Alpha-Mendeleev Rise system.

Acknowledgments

The authors thank the Russian Federal Agency for Mineral Resources for supporting the "Arctic-2012" data acquisition, processing, and interpretation. I. Artemieva acknowledges funding by DFF (Denmark), grant DFF-FNU-1323-00053. Discussions of geological interpretation with S.P. Shokalsky, M.L. Verba, and I.Yu. Vinokurov, and participation of N.V. Smolina in MCS data processing are acknowledged. We are grateful to 2 anonymous reviewers; the manuscript has benefitted from these constructive suggestions. The manuscript was handled by the Associate Editor Dr. Volker Klemann and the Guest Editor Dr. Morten Smerlor.

Appendix A. Seismic data processing

Processing of MCS reflection data

The main goal of the MCS data processing is to constrain a detailed seismic image of the velocity structure and the reflections in the sedimentary cover; the latter introduce significant distortions of the arrival time of main phases in the OBS survey. The velocity analysis of the MCS data is used to model seismic velocities in the sedimentary cover with the maximum possible resolution. The MCS reflection depth-section is constrained by using a combined velocity model, including the results of the velocity analysis of the MCS data for the sedimentary cover and the OBS data for the upper crustal layers.

The MCS seismic data processing (implemented in the Echos processing system of the Paradigm software package) includes a set of standard procedures, such as formation of the common-mid-point

(CMP) line geometry in the coordinate system of the OBS profile, amplitude debiasing, suppression of low-frequency noise by frequency filtering, suppression of multiple waves by the SRME methods; amplitude correction for spherical divergence, suppression of coherent noise based on common shot gathers, ensemble amplitude equalization, an interactive analysis of CMP root-mean-square velocities, spiking deconvolution, normal moveout correction, CMP stacking, velocity modeling for migration based on the CMP velocity field in the sedimentary cover with account for the velocity model for the basement, Kirchhoff post-stack migration, FX-deconvolution, generation of the velocity model for time-to-depth conversion, and time-to-depth conversion. A seismic depth-section for the upper crust along the MCS line combined with interfaces from the OBS data modeling is shown in Fig. 2.

OBS data processing

The main purpose of the OBS data pre-processing is to obtain the maximum number of noise-free seismic records of refracted and wide-angle reflected waves from the boundaries in the crust and the uppermost mantle. P-, S-, and converted PS-waves, due to their different polarizations, manifest themselves differently in the records on hydrophones, vertical and horizontal geophones. We sort the OBS records into common receiver gathers, and apply all necessary technical corrections and assign the proper geometry. Next we process the hydrophone and the vertical components to identify P-waves, and process the horizontal components to identify S- and PS-waves. By “pure” S-waves we mean PS-waves that propagate with transverse polarization along the entire path below the conversion point at the seafloor on the downgoing raypaths.

The processing of the hydrophones records and the vertical component of geophones records includes the following basic procedures: attenuation of reflection wave amplitude, predictive deconvolution, frequency band filtering, and amplitude normalization. Processing records for the horizontal component includes additional steps (besides procedures aimed at attenuation of irregular noise, also applied to P-waves): (1) calculation of the radial and transverse horizontal components by applying a virtual rotation of a seismometer around its vertical axis by a rotation matrix with the directional angles detected from the direct water wave; (2) enhancing S- and PS-waves by suppressing P-waves. Procedures of fan, adaptive, coherent, FK filtering and subtraction of waves with given apparent velocities are widely used. Examples of P-, PS-, and S-waves records are given in Figs. S1–S3.

Appendix A. Supplementary data

Supplementary data associated with this article can be found, in the online version, at https://doi.org/10.1016/j.jog.2018.03.006.

References

Aleinikov, A.L., Nemzorov, N.I., Kashubin, S.N., 1991. Rock Type Determination Method from Seismic Data – Certificate of Authorship N 1642416 A1 Cl. G 01 V1/30. (in Russian).

Austrheim, H., 1987. Eclogitization of lower crustal granulites by fluid migration through shear zones. Earth Planet Sci. Lett. 81, 221–232.

Bohnhoff, M., Makris, J., 2004. Crustal structure of the Southeastern Iceland-Faeroe Ridge (IFR) from wide aperture seismic data. J. Geodyn. 37 (2), 233–252.

Chian, D., Lebedeva-Ivanova, N., 2015. Atlas of Sonobuoy Velocity Analyses in Canada Basin. http://dx.doi.org/10.4095/295857.

Chian, D., Jackson, H.R., Hutchinson, D.R., Shimeld, J.W., Oakey, G.N., Lebedeva-Ivanova, N., Li, Q., Saltus, R.W., Mosher, D.C., 2016. Distribution of crustal types in Canada basin, Arctic Ocean. Tectonophysics 691, 8–30. http://dx.doi.org/10.1016/j.tecto.2016.01.038.

Christensen, N., 1996. Poisson's ratio and crustal seismology. J. Geophys. Res. 101 (B2), 3139–3156.

Coffin, M.F., Eldholm, O., 1994. Large igneous provinces: crustal structure, dimensions, and external consequences. Rev. Geophys. 32, 1–36.

Courtier, A.M., Hart, D.J., Christensen, N.I., 2004. Seismic properties of Leg 195 serpentinites and their geophysical implications. In: In: Shinohara, M., Salisbury, M.H., Richter, C. (Eds.), Proc. ODP, Sci. Results, vol. 195. pp. 1–12.

Dove, D., Coakley, B., Hopper, J., Kristoffersen, Y., 2010. Bathymetry, controlled source seismic and gravity observations of the Mendeleev ridge; implications for ridge structure origin, and regional tectonics. Geophys. J. Int. 183, 481–502.

Forsyth, D., Morel, A.L., Huissier, P., Asudeh, I., Green, A., 1986. Alpha Ridge and iceland-products of the same plume? J. Geodyn. 6, 197–214.

Funck, T., Jackson, H.R., Shimeld, J., 2011. The crustal structure of the Alpha Ridge at the transition to the Canadian Polar Margin: results from a seismic refraction experiment. J. Geophys. Res. Solid Earth 116, 1–26.

Gaina, C., Werner, S.C., Saltus, R., Maus, S., the Camp-GM GROUP, 2011. Circum-Arctic mapping project: new magnetic and gravity anomaly maps of the Arctic. Arctic Petroleum Geology. Geological Society London, Memoirs, 35, pp. 39–48.

Gardner, G.H.F., Gardner, L.W., Gregory, A.R., 1974. Formation velocity and density – the diagnostic basics for stratigraphic traps. Geophysics 29 (No 6), 770–780.

Gottlieb, E.S., Miller, E.L., Andronikov, A.V., Brumley, K., Mayer, L.A., Mukasa, S.B., 2010. Cretaceous Arctic Magmatism: Slab Vs Plume? Or Slab and Plume? AGU Fall Meeting Abstracts 12/2010.

Hyndman, R.D., 1979. Poisson’s ratio in the oceanic crust –a review. Tectonophysics 59, 321–333.

Ito, K., Kennedy, G.C., 1971. An Experimental study of the Basalt-Garnet Granulite-Eclogite Transition. AGU, Geophys. Monogr. Ser. 14, 303–314.

Jackson, H.R., Dahl-Jensen, T., the LORITA working group, 2010. Sedimentary and crustal structure from the Ellesmere Island and Greenland continental shelves onto the Lomonosov Ridge, Arctic Ocean. Geophys. J. Int. 182, 11–35.

Jokat, W., 2003. Seismic investigations along the western sector of Alpha Ridge, Central Arctic Ocean. Geophys. J. Int. 152, 185–201.

Kashubin, S.N., Pavlenkova, N.I., Petrov, O.V., Milshtein, E.D., Shokalsky, S.P., Erinchek, Yu.M., 2013. Crustal types of the circumpolar Arctic. Reg. Geol. Metallogeny 55, 5–20 (in Russian).

Kashubin, S.N., 1984. Analysis procedure of physical rock properties in regional seismic studies (case study of the Tagil-Magnitogorsk Trough). Geophysical Methods of Prospecting and Exploration of Metallic and Non-Metallic Deposits. SGI, Sverdlovsk, pp. 83–91 (in Russian).

Krasovsky, S.S., 1981. The Effect of Continental Crust Dynamics on the Gravity Field. Naukova Dumka, Kiev (in Russian).

Circum-Arctic evolution. In: In: Lane, L.S., Stephenson, R.A. (Eds.), Tectonophysics, vol. 691A (Special Issue.

Lebedev, S., Schaeffer, A.J., Fullea, J., Pease, V., 2017. Seismic Tomography of the Arctic Region: Inferences for the thermal structure and evolution of the lithosphere. Geological Society London Sp. Publ.

Lebedeva-Ivanova, N.N., Zamansky, Y.Y., Langinen, A.E., Sorokin, M.Y., 2006. Seismic profiling across the Mendeleev Ridge at 82°N: Evidence of continental crust. Geophys. J. Int. 165, 527–544.

Lebedeva-Ivanova, N.N., Gee, D.G., Sergeyev, M.B., 2011. Chapter 26 crustal structure of the East Siberian continental margin, Podvodnikov and Makarov basins, based on refraction seismic data (TransArctic 1989–1991). Arctic Petroleum geology.). In: Spencer, Embry, Gautier, Stoupakova, Sørensen (Eds.), Arctic Petroleum Geology. Geological Society of London, N. 35, pp. 395–411.

Miller, E.L., Toro, J., Gehrels, G., Amato, J.M., Prokopiev, A., Tuchkova, M.I., Akinin, V.V., Dumitru, T.A., Moore, T.E., Cecile, M.P., 2006. New insights into Arctic paleogeography and tectonics from U-Pb detrital zircon geochronology. Tectonics 25, 1–19.

Milshtein, E.D., Petrov, B.V., et al., 2008. Development of methodological foundations and technologies for geological interpretation of deep geophysical data along reference and regional lines with the creation of specialized geological mapping products and reassessment of the mineralogical potential of areas. Proceedings of VSEGEI, vol. 7. VSEGEI Publishing House, St. Petersburg, pp. 135–155 (55) (in Russian).

Mjelde, R., Kodaira, S., Sellevoll, M.A., 1996. Crustal structure of the Lofoten Margin N. Norway, from normal incidence and wide-angle seismic data: a review. Norsk Geologisk Tidss krift 76, 187–198.

Morozov, A.F., Petrov, O.V., Shokalsky, S.P., Kashubin, S.N., Kremenetsky, A.A., Shkatov, M.Yu., Kaminsky, V.D., Gusev, E.A., Grikurov, G.E., Rekant, P.V., Shevchenko, S.S., Sergeev, S.A., Shatov, V.V., 2013. New geological data substantiating the continental nature of the region of the Central Arctic uplifts. Reg. Geol. Metallogeny 53, 34–55 (in Russian).

Morozov, A.F., Shkatov, M.Yu., Korneev, O.Yu., Kashubin, S.N., 2014. Combined geological and geophysical expedition Arctic-2012 aimed at grounding the continental nature of the Mendeleev Rise in the Arctic Ocean. Prospect Prot. Min. Res. 3, 22–27 (in Russian).

Oakey, G.N., Saltus, R.W., 2016. Geophysical analysis of the Alpha–Mendeleev ridge complex: characterization of the High Arctic Large Igneous Province. Tectonophysics 691A, 65–84.

Operto, S., Charvis, P., 1995. Kerguelen Plateau: a volcanic passive margin fragment? Geology 23 (2), 137–140.

Petrov, O.M., Morozov, A., Shokalsky, S., Kashubin, S., Artemieva, I.M., Sobolev, N., Petrov, E., Ernst, R.E., Sergeev, S., Smelror, M., 2016. Crustal structure and tectonic model of the Arctic region. Earth Sci. Rev. 154, 29–71. http://dx.doi.org/10.1016/j.earscirev.2015.06.008.

Pollack, H.N., Chapman, D.S., 1977. On the regional variation of heat flow, geotherms and lithospheric thickness. Tectonophysics 38, 279–296.

Poselov, V.A., Kaminsky, V.D., Avetisov, G.P., Pavlenkin, A.D., Andreeva, I.A., Butsenko, V.V., 2007. Deep structure of the continental shelf in the area of the Mendeleev Ridge (Eastern Arctic) based on the results of geological and geophysical studies along the Arctic 2005 reference line. Crust and Upper Mantle Models. VSEGEI Publishing House, pp. 163–167 (in Russian).

Poselov, V.A., Avetisov, G.P., Kaminsky, V.D., 2011. Russian Arctic Geotraverses. FGUP

I.S. Gramberg VNIIOkeangeologia, St. Petersburg (in Russian).
Sakulina, T.S., Verba, M.L., Kashubina, T.V., Krupnova, N.A., Tabyrtsa, S.N., Ivanov, G.I., 2011. Comprehensive geological and geophysical studies along the 5-AR reference line in the East Siberian Sea. Prospect Prot. Min. Res. 10, 17–23 (in Russian).
Thybo, H., Artemieva, I.M., 2013. Moho and magmatic underplating in continental lithosphere. Tectonophysics 609, 605–619.
White, R.S., McKenzie, D.P., 1989. Magmatism at rift zones: the generation of volcanic continental margins and flood basalts. J. Geophys. Res. 94 (685–687), 729.
Zelt, C.A., Smith, R.B., 1992. Seismic traveltime inversion for 2-D crustal velocity structure. Geophys. J. Int. 108, 16–34.